DOI 10.1007/s11182-024-03223-z
Russian Physics Journal, Vol. 67, No. 8, August, 2024

INFLUENCE OF IMPURITIES ON DEFECT FORMATION AND OXYGEN DIFFUSION IN TiN

A. V. Bakulin and S. E. Kulkova UDC 544.034

The effect of substitutional impurities on the formation energy of nitrogen vacancies and the oxygen defect on the N-sublattice as well as on the oxygen migration energy in TiN *is studied using the projector augmented wave method. It has been shown that 4d transition metals with the exception of* Zr *and elements of IIIA and IVA groups excluding* Al *and* Si *reduce the formation energy of nitrogen vacancies. At the same time, regardless of the impurity, the formation energy of the oxygen defect has a negative value. The oxygen migration energy within the first coordination sphere is increased by almost all impurities, while metals of the middle of the 4d-period slightly lower the migration barrier of oxygen, which allows it to move away from the impurity atom. The lower and upper limits of the temperature-dependent diffusion coefficient of oxygen in the doped titanium nitride are estimated. It has been revealed that almost all considered impurities reduce the diffusion coefficient mainly due to a change in the migration energy.*

Keywords: diffusion, titanium nitride, oxygen, impurity, electronic structure.

INTRODUCTION

Titanium nitride is a material of great technological importance because of its extreme hardness, wear resistance, chemical stability, high melting point, golden color, metallic conduction, good thermal and electrical conductivity, as well as biocompatibility [1–5]. It has many special uses ranging from reflect and hard coatings to microelectronic devices [6–7]. Titanium nitride films can be formed at the oxide–substrate interfaces during the oxidation of titanium and its alloys due to the nitrogen penetration into the oxidation region from the atmosphere. For example, the formation of the TiN layers at such interfaces observed in works [8, 9], according to the authors' opinion, leads to an increase in the titanium oxidation resistance. A similar conclusion was made in works [10–13], where the oxidation of Ti–Al alloys was considered. It is believed that TiN acts as a diffusion barrier, slowing down the oxygen penetration into the alloy and the oxide growth.

It is well known that to improve the oxidation resistance of the γ-TiAl alloy, different techniques are used including alloying with one or more elements (see works [14–17] and references therein). Most authors agreed that Nb, Ta, W, and Si are the most suitable elements for increasing the oxidation resistance of this alloy [17]. However, the results of different studies are often contradictory regarding the effect of the same impurities on the oxidation resistance. During the oxidation process, alloying elements can either remain in the alloy or incorporate into the resulting titanium nitride and oxide scale. The presence of impurities in TiN, which replace titanium, can affect its stability, the concentration of defects, as well as the oxygen diffusivity. In our previous work [18], the oxygen diffusion in pure TiN was studied within vacancy and interstitial mechanisms. It was shown that, depending on the chemical potential of nitrogen and oxygen, the temperature-dependent diffusion coefficient (D) of the latter in TiN varies in a wide range, but remains higher than that in Al_2O_3 and is comparable to the oxygen diffusion coefficient in TiO_2. The effect of substitutional impurities on the oxygen diffusion in TiN has not been previously studied.

Institute of Strength Physics and Materials Science of the Siberian Branch of the Russian Academy of Sciences, Tomsk, Russia, e-mail: bakulin@ispms.ru; kulkova@ispms.ru. Original article submitted June 28, 2024.

It is well known that experimental study of the impurity diffusion requires solving a number of problems related to the purity of samples, the capabilities of indicator elements, surface oxidation, etc. Experimental study of the mechanisms of atomic diffusion is difficult or even impossible. In addition, there is a significant scatter in the experimental values of the temperature-dependent diffusion coefficient and activation energy (Q). At the same time, modern methods for calculating the electronic structure within the density functional theory [19] in combination with the transition state theory [20] make it possible to estimate the diffusion coefficient in various materials with sufficient accuracy. Thus, the main goal of this work is theoretical study of the effect of substitutional impurities on the formation energy of point defects in TiN, which are necessary for oxygen diffusion, and on the oxygen temperature-dependent diffusion coefficient.

1. COMPUTATIONAL DETAILS

Atomic and electronic structures of ideal and defective TiN were calculated by the projector augmented-wave (PAW) method [21, 22] in the plane wave basis. We used the generalized gradient approximation (GGA) for the exchange-correlation with Perdew–Burke–Ernzerhof (PBE) functional [23]. The cutoff energy of the plane waves from the basis set was 550 eV. Optimization of the atomic structure of the defective titanium nitride was carried out using the conjugate gradient method with accuracy of ~0.01 eV/Å. Titanium nitride has a NaCl-type structure (space group $Fm\bar{3}m$ No. 225). The equilibrium lattice parameter, equal to 4.255 Å, differs from the experimental value of 4.238 Å [24] by ~0.4%. To study the effect of substitutional impurities on the defect formation energy in TiN, the cubic supercell (3 × 3 × 3) containing 216 atoms was used. Integration over the Brillouin zone was carried out using a 5 × 5 × 5 k-point grid generated by the Monkhorst–Pack scheme [25]. Test calculations showed that the use of a finer k-point grid leads to a change in the total energy of the system within 1.5 meV/atom.

The formation heat of the doped titanium nitride per formula unit was estimated using the following formula:

$$H^{\mathrm{f}} = \left[E(\mathrm{TiN}+\mathrm{Me}) - 107E(\mathrm{Ti}) - E(\mathrm{Me}) - 108E(\mathrm{N}_2)/2\right]/108\,, \tag{1}$$

where E(TiN + Me) is the total energy of the doped TiN supercell; E(Ti) and E(Me) are the energies of titanium and impurity in the ground state per atom; $E(\mathrm{N}_2)$ is the energy of an isolated nitrogen molecule, calculated in the empty cell of size 15 × 15 × 15 Å^3. The numerical coefficients in Eq. (1) are determined by the size of the supercell and the fact that an impurity atom occupies a Ti position.

The formation energies of a nitrogen vacancy ($\mathrm{V_N}$) and an oxygen defect ($\mathrm{O_N}$) on the N-sublattice were estimated using the following formulas:

$$E^{\mathrm{f}}(\mathrm{V_N}) = E(\mathrm{TiN}+\mathrm{V_N}) + 1/2E(\mathrm{N}_2) - E(\mathrm{TiN}) \tag{2}$$

and

$$E^{\mathrm{f}}(\mathrm{O_N}) = E(\mathrm{TiN}+\mathrm{O_N}) - 1/2E(\mathrm{O}_2) + 1/2E(\mathrm{N}_2) - E(\mathrm{TiN})\,, \tag{3}$$

where $E(\mathrm{TiN}+\mathrm{V_N})$ and $E(\mathrm{TiN}+\mathrm{O_N})$ are the total energies of the TiN supercell with the vacancy and the oxygen defect, respectively; E(TiN) is the energy of the ideal titanium nitride; $E(\mathrm{O}_2)$ is the energy of an isolated oxygen molecule, calculated in the same way as $E(\mathrm{N}_2)$. The interaction energy of any two defects (X and Y) was estimated as

$$E^{\mathrm{int}}(\mathrm{X}-\mathrm{Y}) = E(\mathrm{TiN}+\mathrm{X}+\mathrm{Y}) - E(\mathrm{TiN}+\mathrm{X}) - E(\mathrm{TiN}+\mathrm{Y}) + E(\mathrm{TiN})\,, \tag{4}$$

where E(TiN + X + Y) and E(TiN + X/Y) are the total energies of the TiN supercell with two and one defect, respectively. According to Eq. (4), a positive value of E^{int} indicates the repulsion interaction between the defects, and

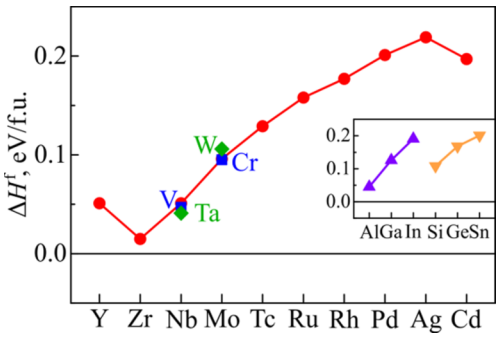

Fig. 1. Changes in the formation heat of TiN after doping.

a negative value means their attraction. The overlap population and charge transfer between atoms in TiN was estimated using the density derived electrostatic and chemical (DDEC6) method [26].

2. RESULTS AND DISCUSSION

The change in the TiN formation heat upon doping is shown in Fig. 1. It can be seen that all considered impurities increase the formation heat of TiN reducing its thermodynamic stability, while zirconium has the least effect on H^f. This result is typical for compounds with ionic-covalent bonds, such as oxides, nitrides, etc., and for their interfaces (for example, see works [27, 28]), since impurities induce a local distortion of the atomic structure and the electron density distribution; the farther an impurity element is located from Ti in the periodic table, the stronger its influence. The isoelectronic elements of the VB and VIB groups have almost the same effect on the formation heat of TiN. At the same time, a more pronounced effect of the IVA group elements compared to the IIIA group ones is due to both their higher valence and electronegativity. Note that the electronegativity of all considered *s*, *p*-elements is higher than that of titanium. In the series of isoelectronic elements of the IIIA and IVA groups, ΔH^f growth with increasing impurity period is due to the weakening of the Me-*s*, *p*–N-*p* interaction compared to Ti-*d*–N-*p*.

Local densities of electronic states (DOS) of some impurities as well as the nearest nitrogen atoms, in comparison with those of titanium and nitrogen in the ideal TiN, are shown in Fig. 2. Figure 2*a* shows that the main peak of the occupied part of the Y valence band is shifted toward the Fermi level (E_F) compared to its position on the Ti DOS, which is also reflected in the shift of the peak of the nitrogen valence band. The positions of the DOS peaks in the occupied part of the valence band of Zr and Ti are in good agreement (Fig. 2*b*), and with the filling of the *d*-band of the impurity, these peaks shift toward low energies (Fig. 2*c*–*f*). At the same time, in the case of metals of the second half of the 4*d* period, the main peak of the nitrogen DOS remains at the same energies as in undoped titanium nitride, and these impurities induce new peaks located both closer to the Fermi level and farther from it (Fig. 2*e* and *f*). For example, substitution of titanium by rhodium leads to the appearance of a peak in the N DOS at energies of –5.8 and –2.0 eV (Fig. 2*e*), at which the sharp Rh peaks are located. The interaction of nitrogen with silver leads to the appearance of three new peaks on the DOS curve of the latter (Fig. 2*f*). Besides, substitution of titanium also causes some distortion of the TiN atomic structure: in the case of 4*d* metals, the displacement of the nitrogen atoms closest to the impurity away from it first decreases from 0.10 Å (Y) to 0.03 Å (Ru), and then increases to 0.12 Å (Ag and Cd). Note that such change in the Me–N bond length is consistent with a change in the lattice parameter of 4*d* metal mononitrides [29].

The formation energies of a nitrogen vacancy near a substitutional impurity are shown in Fig. 3. It can be seen that almost all transition metal impurities with the exception of Zr reduce the formation energy of the N-vacancy, which is consistent with an increase in H^f. As the *d* band of the impurity is filled, the Me–N interaction becomes weaker that leads to a stronger decrease in $E^f(V_N)$. In the case of *s*, *p*-elements, a more pronounced change in the vacancy formation energy with increasing impurity period also correlates with the change of the formation heat of titanium nitride. At the same time, the increase in $E^f(V_N)$ caused by Al and Si is due to a combination of structural and electronic factors. In both cases, the substitution of titanium causes a displacement of the nearest nitrogen atoms by 0.07–0.16 Å toward the

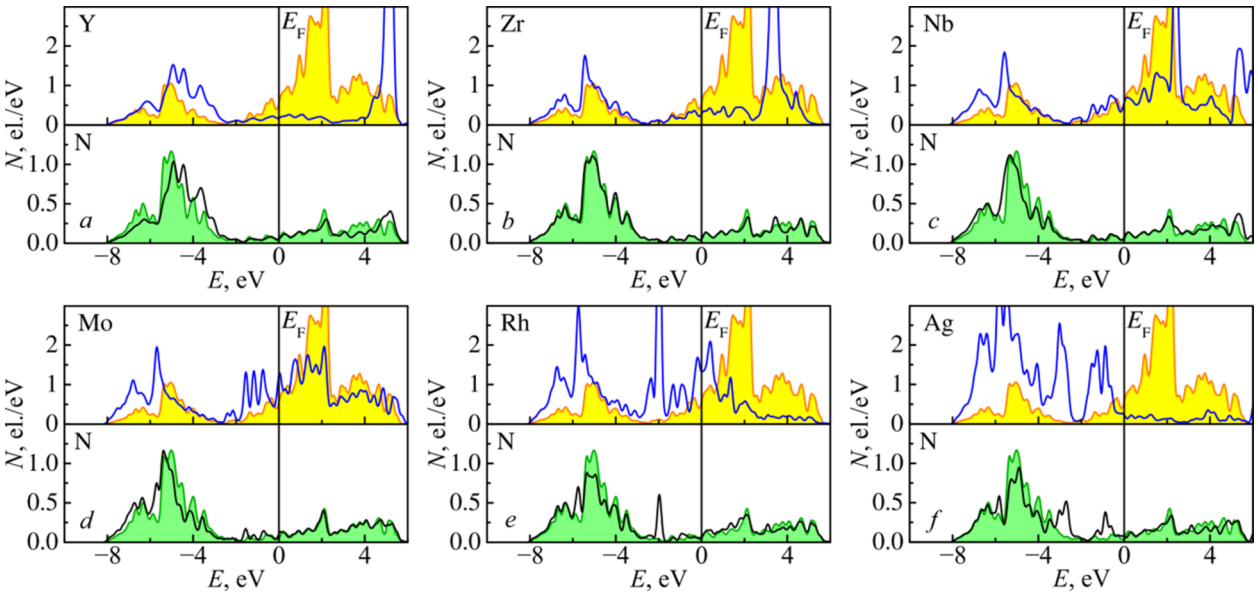

Fig. 2. Local densities of electronic states of some impurities of 4*d* metals and the nearest N atoms in comparison with the DOS of Ti and N in the ideal titanium nitride shown by filling.

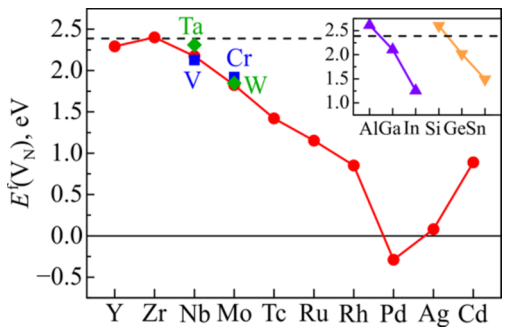

Fig. 3. Formation energy of the nitrogen vacancy near the impurity atom. The horizontal dashed line corresponds to the value obtained for undoped TiN.

impurity atom, which enhances the Me–N interaction. The electronic mechanism for strengthening these bonds depends on the impurity group. In particular, the aluminum atom gives up 0.17 el. larger than titanium that enhances the bond ionicity, while the overlap population of the Al–N bond is 0.08 el. lower than Ti–N. On the contrary, in the case of silicon, the overlap population of the Si–N bond increases by 0.09 el., and the charge transfer from the Si atom to N decreases by 0.08 el.

It should be noted that the formation of the nitrogen vacancy in the second coordination sphere (CS) of an impurity atom requires almost the same energy as in the case of undoped TiN. The maximum decrease in $E^f(V_N)$ for Pd is only 0.10 eV, so we can assume that the impurity effect does not extend beyond the first CS. In general, the obtained results from the viewpoint of their influence on the oxygen diffusivity can be interpreted in two ways: on the one hand, almost all impurities contribute to the formation of nitrogen vacancies in their local environment, thereby increasing the average concentration of the vacancies in TiN, which is favorable for the oxygen diffusion along the N sublattice; on the other hand, impurities create a potential well for a vacancy, the depth of which is equal to the change in its formation energy, and since diffusion proceeds through the vacancy mechanism, the oxygen atom can be trapped by the impurity.

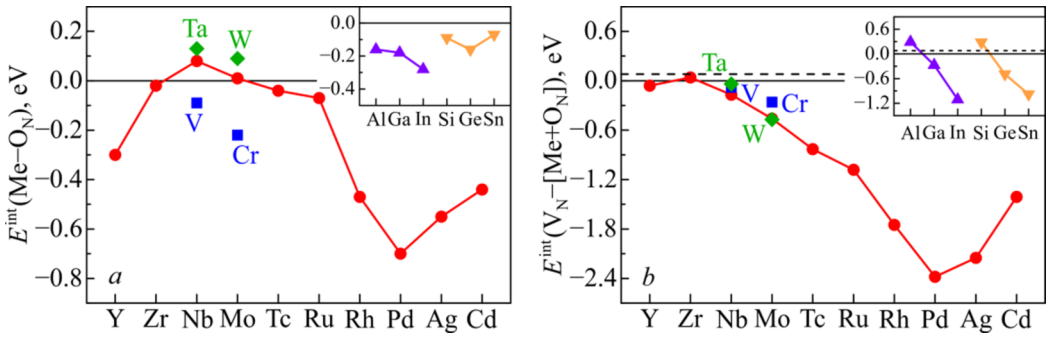

Fig. 4. Interaction energy between the impurity and oxygen (*a*) as well as nitrogen vacancy and the *impurity* + *oxygen* complex (*b*). The horizontal dashed line shows the value obtained for undoped TiN.

As was shown in our previous work [18], depending on the specific values of the chemical potential of oxygen and nitrogen in TiN, both interstitial and vacancy mechanisms of oxygen diffusion can dominate. In this case, the diffusion coefficient corresponding to the vacancy mechanism changes over a wider range. In this regard, below we discuss the influence of substitution impurities only on those energy characteristics that need for estimation of the temperature-dependent diffusion coefficient of oxygen over the N sublattice. For example, some impurities, due to the Me–O interactions, can locally slow down or accelerate the oxygen diffusion in titanium nitride.

Figure 4*a* shows the calculated interaction energies between the impurities and oxygen located in the nearest position on the N sublattice. It can be seen that almost all considered impurities, with the exception of Nb, Mo, and their isoelectronic elements Ta and W, attract oxygen. The character of the interaction depends on the specific element, but in general is determined by the competition of structural and electronic factors. For example, in the case of Y and Zr, despite their atomic radii are larger than the Ti atomic radius, the Me–O bond length decreases only slightly (by 0.01–0.02 Å) compared to the Ti–O bond length, which compensates the lattice expansion caused by the replacement of titanium by these impurities. Although the radii of Ag and Cd are also larger than the titanium radius, they interact weakly with oxygen, which leads to an increase in the Me–O bond length (by 0.14–0.17 Å) and a decrease in the Me–N and Ti–O bond lengths (by 0.04–0.12 Å). Note that the 4*d* metal atoms from Tc to Pd, as well as V and Cr, are smaller than titanium, but the Me–O bond length is larger than Ti–O in undoped TiN. Thus, the strengthening of the interaction between Me–N and Ti–O is sufficient to compensate for the weakening of Me–O relative to Me–N upon doping with the elements mentioned above. Moreover, from the viewpoint of the interaction energy calculated by Eq. (4), the impurity and oxygen interact attractively. Positive values of the Me–O interaction energy in the case of Nb, Mo, Ta, and W are explained by a more significant enhancement of the Me–N interaction in doped TiN compared to similar bonds in the presence of oxygen or with Ti–N in ideal titanium nitride. This leads to an increase in E^{int}(Me–O). It can be concluded that those impurities for which $E^{int} < 0$ can trap oxygen, thereby slowing down its average diffusion rate. At the same time, impurities with positive value of the interaction energy create a region into which oxygen does not diffuse. Therefore, such elements should have virtually no effect on the oxygen diffusion rate by changing the migration energy.

As can be seen from Fig. 4*b*, the interaction energy of the nitrogen vacancy with an *impurity* + *oxygen* complex is also negative for the most impurities. Positive values of E^{int} were obtained only for Zr (0.04 eV), Al (0.29 eV), and Si (0.28 eV). Note that in the case of undoped TiN, this energy is also positive and equals to 0.08 eV (the dashed line in Fig. 4*b*). The repulsion between the nitrogen vacancy and Al/Si atoms, found in TiN without oxygen (E^{int} = 0.23/0.21 eV), is not only maintained in the presence of oxygen, but also increases by 0.06/0.07 eV, respectively.

Let us discuss changes in the migration energy of oxygen near thee impurity atom. There are two possible options: 1) the initial and final positions are located in the first neighbors of the impurity atom; 2) only the initial position of oxygen is located near the impurity. Figure 5*a* shows that in the first case, all considered impurities, except V, Cr, Al, and Si, increase the oxygen migration barrier, but the effect of *d*3–*d*6 impurities is less pronounced. In spite of the fact that Al and Si reduce the migration energy, their isoelectronic elements increase it. In general, the change in

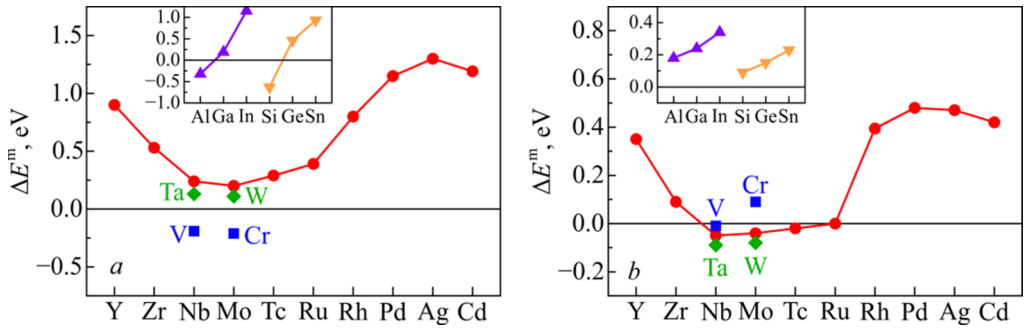

Fig. 5. Change in the oxygen migration energy: the initial and final positions are in the first neighbors of the impurity atom (*a*), and only the initial position of oxygen lies near the impurity (*b*).

the migration energy of oxygen within the first coordination sphere of the impurity atom (Fig. 5*a*) correlates with the change in the Me–O interaction energy (Fig. 4*a*): an increase in the attractive interaction induces the increase of the migration barrier. The effect of titanium substitution impurities on the oxygen migration energy from the first to the second neighbors has of a slightly different character (Fig. 5*b*): only Nb, Mo, Tc, Ta, and W lower the barrier, the effect of Ru and V is negligible, and all other considered elements increase the migration energy. In general, the influence of the impurities on the oxygen migration barrier from the first to the second neighbors of the impurity atom is less pronounced than that within the first CS.

To estimate the diffusion coefficient in doped TiN, we take advantage of the method proposed in our previous work [18] and consider two cases: 1) there are only thermal vacancies TiN_1, and 2) there are the constitutional vacancies $TiN_{0.6}$. Recall that the maximum deviation from stoichiometry at which TiN with the NaCl-type structure is stable corresponds to the $TiN_{0.6}$ composition [30]. It should be emphasized that the presence of the constitutional vacancies is reflected only on the estimation of the total nitrogen vacancy concentration. All other characteristics are the same in both approximations. The average value of the migration energy can be calculated as the weighted arithmetic mean of the values obtained for ideal and doped TiN. The weights depend on the impurity concentration. It is supposed that the atomic concentration of the impurity is equal to c_0, and the impurity atoms are uniformly distributed in the bulk. Let us select a certain volume of the crystal including only one impurity atom. Such volume contains $1/c_0$ unit cells of TiN or $1/(2c_0)$ sites on the N sublattice. Only six sites of them are located on the first coordination sphere, the rest sites are located on the second CS or even farther. From each of these six sites, four jumps allow oxygen to remain on the first CS, four jumps allow O to move to the second CS, and other four jumps allow it to be in sites more distant from the impurity atom. Thus, only 24 atomic jumps from $12/(2c_0)$ occur in the selected volume within the first CS, 48 jumps allow for oxygen to move from the first CS to second CS or even farther, and $(6/c_0 - 72)$ atomic jumps occur far from the impurity. As a result, the average migration energy can be estimated as

$$\left\langle E^{\mathrm{m}} \right\rangle = 4c_0 \left[E^{\mathrm{m}}(1) + 2E^{\mathrm{m}}(2) \right] + (1 - 12c_0) E^{\mathrm{m}}(0), \tag{5}$$

where $E^{\mathrm{m}}(1)$ and $E^{\mathrm{m}}(2)$ are the oxygen migration energies within the first CS and from the first to second CS or even farther, respectively; $E^{\mathrm{m}}(0)$ is the oxygen migration energy in undoped TiN. The range of applicability of this model corresponds to the positive value of the expression in parentheses on the right side of Eq. (5), i.e. $c_0 \le 8.33$ at.%. All numerical estimates are given below for a substitutional impurity concentration equal to 5 at.%. For convenience, Eq. (5) can be rewritten in terms of changes in the migration energy shown in Fig. 5:

$$\left\langle E^{\mathrm{m}} \right\rangle = 4c_0 \left[\Delta E^{\mathrm{m}}(1) + 2\Delta E^{\mathrm{m}}(2) \right] + E^{\mathrm{m}}(0). \tag{6}$$

The average oxygen jump rate for each impurity is calculated using the following formula:

$$\langle \Gamma \rangle = \sqrt{\frac{\langle E^{\mathrm{m}} \rangle}{2ml^2}} \exp\left(-\frac{\langle E^{\mathrm{m}} \rangle}{k_{\mathrm{B}} T} \right), \tag{7}$$

where m is the mass of the diffusing atom, l is the jump length, k_{B} is the Boltzmann constant, and T is the temperature. Note that the numerator of the exponent must include the sum of the formation energy of the defect providing the O diffusion and the migration energy. However, as noted above, the energy of replacing nitrogen with oxygen is negative for all impurities; therefore, its effective value is equal to zero.

We now estimate similarly the average value of the formation energy of the nitrogen vacancy: four of the $1/(2c_0)$ nitrogen sites are located near the impurity and the oxygen atom; therefore, the vacancy formation energy is equal to the sum of its value in undoped TiN and the interaction energy with the *impurity* + *oxygen* complex: $E^{\mathrm{f}}(\mathrm{V_N}) + E^{\mathrm{int}}(\mathrm{V_N} - [\mathrm{Me} + \mathrm{O_N}])$; four sites are located near oxygen and in the second neighbors of the impurity atom, and the remaining four sites are far from the impurity. For the last two groups, the influence of the impurity can be neglected, and the vacancy formation energy is estimated as $E^{\mathrm{f}}(\mathrm{V_N}) + E^{\mathrm{int}}(\mathrm{V_N} - \mathrm{O_N})$. Thus, the average value of the formation energy of the nitrogen vacancy is equal to the following expression:

$$\left\langle E^{\mathrm{f}}(\mathrm{V_N}) \right\rangle = \frac{2}{3} c_0 \left[E^{\mathrm{int}}(\mathrm{V_N} - [\mathrm{Me} + \mathrm{O_N}]) + 2E^{\mathrm{int}}(\mathrm{V_N} - \mathrm{O_N}) \right] + E^{\mathrm{f}}(\mathrm{V_N}). \tag{8}$$

Taking into account the above-mentioned formation energy of the nitrogen vacancy near the impurity, $E^{\mathrm{f}}(\mathrm{V_N})_{\mathrm{Me}}$ shown in Fig. 3, Eq. (8) can be rewritten in the following form:

$$\left\langle E^{\mathrm{f}}(\mathrm{V_N}) \right\rangle = \frac{2}{3} c_0 \left[E^{\mathrm{int}}(\mathrm{V_N} - [\mathrm{Me} + \mathrm{O_N}]) + 2E^{\mathrm{f}}(\mathrm{V_N})_{\mathrm{Me}} \right] + \left(1 - \frac{4}{3} c_0 \right) E^{\mathrm{f}}(\mathrm{V_N}). \tag{9}$$

Recall that the formation energy of the nitrogen vacancy in undoped TiN is 2.34 eV [18]. In the case of TiN_1, the total vacancy concentration is equal to

$$\langle c(\mathrm{V_N}) \rangle = \exp\left(\frac{\langle S^{\mathrm{f}}(T) \rangle}{k_{\mathrm{B}}} \right) \exp\left(-\frac{\langle E^{\mathrm{f}}(\mathrm{V_N}) \rangle}{k_{\mathrm{B}} T} \right), \tag{10}$$

where $\langle S^{\mathrm{f}}(T) \rangle$ is the average value of the formation entropy of the vacancy calculated using a formula similar to Eq. (9). In the case of $TiN_{0.6}$, the thermal vacancies can be neglected, since their concentration is several orders of magnitude lower. Therefore, we assume that $\langle c(\mathrm{V_N}) \rangle = 0.4$.

In general, the oxygen diffusion coefficient for single-jump mechanisms is calculated by the formula:

$$D = fc\Gamma \frac{1}{Z} \sum_{i=1}^{Z} d_i^2, \tag{11}$$

where f is the correlation factor, c is the concentration of defects providing the diffusion, Γ is the jump rate, d_i are the lengths of the projection of the ith jump onto the selected direction, and Z is the number of possible jumps from the initial site. Since the N sublattice forms an fcc structure, and we estimate the oxygen diffusion coefficient along the <100> direction, then $f = 0.78145$ [31], $Z = 12$, and $d_i = a/2$ (a is the lattice parameter) for eight jumps and 0 for other four jumps. The values of other quantities of Eq. (11) must be averaged. Thus, the final expression for the oxygen diffusion coefficient along the <100> direction in doped titanium nitride has the following form:

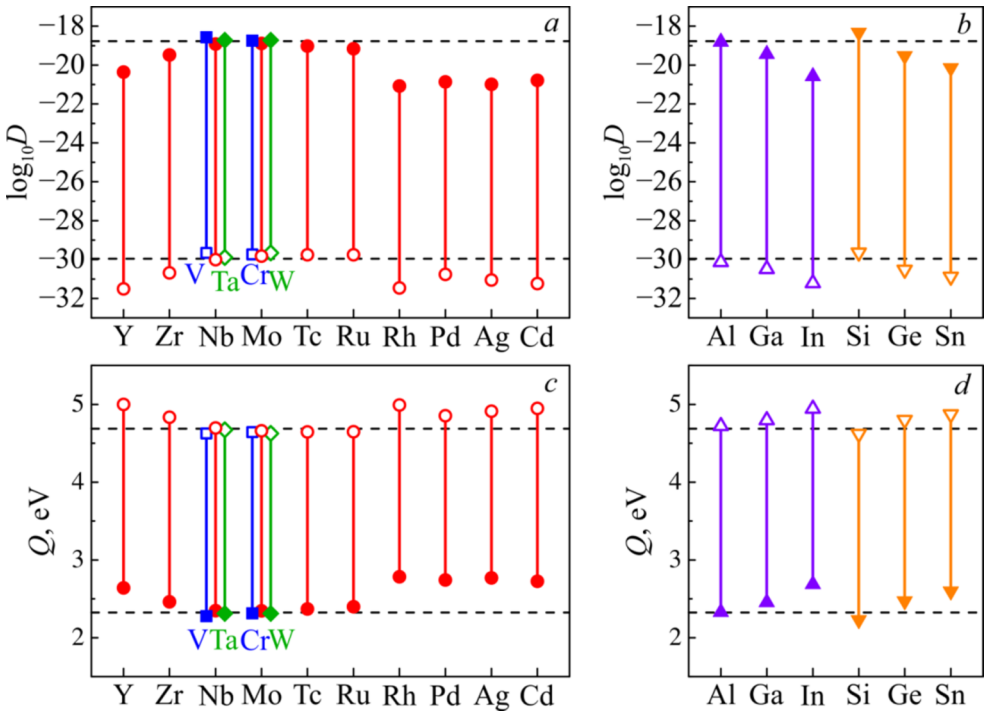

Fig. 6. Upper and lower limits of the change in the temperature-dependent diffusion coefficient of oxygen in doped TiN at 1000 K (*a* and *b*) and of the corresponding activation energy (*c* and *d*). Open and closed symbols show the values calculated for TiN_1 and $TiN_{0.6}$, respectively.

$$D = 0.13a^2 \langle c(V_N) \rangle \langle \Gamma \rangle . \quad (12)$$

Figure 6*a* and *b* shows the interval of change in the oxygen diffusion coefficient in doped TiN at 1000 K. The lower limit corresponds to TiN_1, whereas the upper limit is for $TiN_{0.6}$. It can be seen that the impurities at the beginning and end of the 4*d* period (Y and Zr and Rh, Pd, Ag, and Cd) reduce the diffusion coefficient, while the effect of V, Cr, Nb, Mo, Tc, Ru, Ta, and W is less pronounced. The impurities of the *s*, *p*-elements also predominantly reduce the oxygen diffusivity, only Si slightly increases it, and Al has practically no effect. A comparison of Figs. 6 and 5 demonstrates that the change in *D* correlates with that of the migration barrier. Thus, if the impurity increases, the migration barriers in its first CS, then it can trap diffusing oxygen, thereby reducing the average migration rate and diffusion coefficient. This conclusion is valid for metals at the beginning and end of the 4*d* period and the *s*, *p*-elements such as Ga, In, Ge, and Sn. The impurities of VB–VIIB groups, as well as Al and Ga, have the opposite effect on the oxygen migration barrier within the first coordination sphere of the impurity and when oxygen jumps from the first CS to the second or more distant spheres (Fig. 5). The competition of these factors leads to minor changes in the diffusion coefficient (Fig. 6*a* and *b*). The values of the activation energy of the oxygen diffusion in the doped TiN are shown in Fig. 6*c* and *d*. Since *D* is mainly determined by the activation energy rather than the pre-exponential factor, the decrease/increase in *D* is consistent with the increase/decrease in *Q*.

CONCLUSIONS

For the first time, the oxygen diffusion in doped TiN has been studied by the projector augmented-wave method in combination with the transition state theory. The upper and lower limits of the change in the temperature-

dependent diffusion coefficient were estimated. Calculations of the formation energy of the nitrogen vacancy showed that all 4*d* metals, including V, Nb, Ta, and W as well as Ga, In, Ge, and Sn are beneficial for its decrease. Metals at the end of the 4*d* period decrease $E^{f}(V_N)$ more significantly than others, and in the case of Pd, this energy becomes negative. In addition, the isoelectronic elements of the IIIA and IVA groups lead to a larger decrease in the formation energy of the nitrogen vacancy with increase of their period. At the same time, the effect of Zr is negligible. Similarly, for almost all considered impurities, there is the attractive interaction between the impurity and oxygen as well as between the nitrogen vacancy and the *impurity + oxygen* complex. The estimation of the oxygen migration barriers showed that most impurities led to their increase. When oxygen diffuses within the first coordination sphere of the impurity, only V, Cr, Al, and Si are beneficial to an increase in the migration energy. In the case of oxygen diffusion from the first neighbors of the impurities to the second or more distant ones, the migration energy is reduced by V, Nb, Ta, Mo, and Tc, but the effect of Rh is negligible. The values of the temperature-dependent diffusion coefficient of oxygen were estimated at an impurity concentration of 5 at.% in TiN_1 and $TiN_{0.6}$. It was established that changes in the oxygen diffusivity correlated with those in the migration barrier near the impurity: almost all impurities reduced the diffusion coefficient and increased the activation energy. The greatest effects on *D* and *Q* were found in the case of Y, Rh, Pd, Ag, Cd, In, and Sn.

COMPLIANCE WITH ETHICAL STANDARDS

Author contributions

A.V.B.: developed the statistical model for averaging the diffusion characteristics in doped TiN, performed calculations, discussed the results, contributed to visualization, and wrote the manuscript; S.E.K.: performed conceptualization, calculations, and analysis of the electronic structure, discussed the results, and wrote the manuscript. All authors have read and agreed to the published version of the manuscript.

Conflicts of interest

The authors declare that they have no known competing financial interests or personal relationships that could have appeared to influence the work reported in this paper.

Funding

The work was performed according to the Government Research Assignment for the ISPMS SB RAS (Project FWRW-2022-0001).

Financial interests

The authors have no relevant financial or non-financial interests to disclose.

Institutional review board statement

Applicable.

REFERENCES

1. D. Starosvetsky and I. Gotman, Biomaterials, **22**, 1853–1859 (2001); https://doi.org/10.1016/S0142-9612(00)00368-9.
2. M. Hoseini, A. Jedenmalm, and A. Boldizar, Wear, **264**, 958–966 (2008); https://doi.org/10.1016/ j.wear.2007.07.003.
3. S. V. Ovchinnikov, A. D. Korotaev, V. Yu. Moshkov, and D. P. Borisov, Russ. Phys. J., **54**, 951–964 (2012); https://doi.org/10.1007/s11182-012-9709-5.
4. V. M. Kuznetsov, S. V. Ovchinnikov, and V. A. Slabodchikov, Russ. Phys. J., **61**, 2001–2011 (2019); https://doi.org/10.1007/s11182-019-01630-1.
5. V. M. Savostikov, Yu. A. Denisova, V. V. Denisov, *et al*., Russ. Phys. J., **64**, 2219–2224 (2022); https://doi.org/10.1007/s11182-022-02580-x.
6. B. Gao, X. Li, K. Ding, *et al*., J. Mater. Chem. A, **7**, 14–37 (2019); https://doi.org/10.1039/c8ta05760e.
7. U. Mahajan, M. Dhonde, K. Sahu, *et al*., Mater. Adv., **5**, 846–895 (2024); https://doi.org/10.1039/d3ma00965c.
8. D. Vojtěch, H. Čížová, K. Jurek, and J. Maixner, J. Alloys Compd., **394**, 240–249 (2005); https://doi.org/10.1016/j.jallcom.2004.11.019.
9. A. Kanjer, V. Optasanu, M. C. M. de Lucas, *et al*., Surf. Coat. Technol., **343**, 93–100 (2018); https://doi.org/10.1016/ j.surfcoat.2017.10.065.
10. L. Zhang, J. Wu, K. Jiang, and F. Wang, MRS Online Proc. Library, **552**, 881 (1998); https://doi.org/10.1557/PROC-552-KK8.8.1.
11. J. S. Wu, L. T. Zhang, F. Wang, *et al*., Intermetallics, **8**, 19–28 (2000); https://doi. org/10.1016/S0966-9795(99)00062-X.
12. T. G. Avanessian, Features of high-temperature oxidation and microarc oxidation of alloys based on γ-TiAl [in Russian], Cand. Chem. Sci., Dissertation, NUST MISIS, Moscow (2014).
13. J. Rakowski, D. Monceau, F. S. Pettit, and G. H. Meier, in: Proc. of the Second Int. Conf. on the Microscopy of Oxidation, Institute of Materials, London (1993).
14. J. Dai, J. Zhu, C. Chen, and F. Weng, J. Alloys Compd., **685**, 784–798 (2016); https://doi.org/10.1016/j.jallcom.2016.06.212.
15. D. Vojtěch, T. Popela, J. Kubásek, *et al*., Intermetallics, **19**, 493–501 (2011); https://doi.org/10.1016/j.intermet.2010.11.025.
16. X. Y. Li, S. Taniguchi, Y. Matsunaga, *et al*., Intermetallics, **11**, 143–150 (2003); https://doi.org/10.1016/S0966-9795(02)00193-0.
17. T. Izumi, T. Yoshioka, S. Hayashi, and T. Narita, Intermetallics, **9**, 547–558 (2001); https://doi.org/10.1016/S0966-9795(01)00023-1.
18. A. V. Bakulin, L. S. Chumakova, and S. E. Kulkova, Phys. Mesomech. (in print).
19. P. Hohenberg and W. Kohn, Phys. Rev., **136**, B864–B871 (1964); https://doi.org/10.1103/ PhysRev.136.B864.
20. M. J. Gillan, J. Phys. C: Solid State Phys., **20**, 3621–3641 (1987); https://doi.org/10.1088/0022-3719/20/24/005.
21. P. E. Blochl, Phys. Rev. B, **50**, 17953–17979 (1994); https://doi.org/10.1103/PhysRevB.50.17953.
22. G. Kresse and D. Joubert, Phys. Rev. B, **59**, 1758–1775 (1999); https://doi.org/10.1103/PhysRevB. 59.1758.
23. J. P. Perdew, K. Burke, and M. Ernzerhof, Phys. Rev. B, **77**, 3865–3868 (1996); https://doi.org/10.1103/PhysRevLett.77.3865.
24. N. Schönberg, Acta Chem. Scand., **8**, 213–220 (1954); https://doi.org/10.3891/acta.chem.scand.08-0213.
25. H. J. Monkhorst and J. D. Pack, Phys. Rev. B, **13**, 5188–5192 (1976); https://doi.org/10.1103/PhysRevB.13.5188.
26. T. A. Manz and N. G. Limas, PSC Adv., **6**, 47771–47801 (2016); https://doi.org/10.1039/ C6RA04656H.
27. F. P. Ping, Q. M. Hu, A. V. Bakulin, *et al*., Intermetallics, **68**, 57–62 (2016); https://doi.org/10.1016/j.intermet.2015.09.005.

28. A. V. Bakulin, A. S. Kulkov, and S. E. Kulkova, J. Exp. Theor. Phys., **137**, 362–371 (2023); https://doi.org/10.1134/S1063776123090030.
29. R. de Paiva, R. A. Nogueira, and J. L. A. Alves, Phys. Rev. B, **75**, 085105 (2007); https://doi.org/10.1103/PhysRevB.75.085105.
30. I. Khidirov, Russ. J. Inorg. Chem., **56**, 298–303 (2011); https://doi.org/10.1134/ S0036023611020100.
31. A. Paul, T. Laurila, V. Vuorinen, and S. V. Divinski, Thermodynamics, Diffusion and the Kirkendall Effect in Solids, Springer, Cham (2014).